

Enhancement of nonlinear optical responses of multipole-type excitons by short pulse excitation

Takashi Kinoshita and Hajime Ishihara

Department of Physics and Electronics, Osaka Prefecture University, Sakai, Osaka 599-8531, Japan

(Dated: December 9, 2024)

We theoretically investigate the anomalous optical responses of multicomponent excitons in a thin film where excitonic center-of-mass motions are confined. Taking the A and B excitons of ZnO, we revealed that the large interaction volume between multipole-type excitons and the radiation leads to a large radiative coupling of excitons from different valence-bands. Accordingly, particular exciton–radiation coupled states exhibit the radiative width over 50 meV and radiative decay time reaching several femto-seconds, and thus dominantly survives in the optical spectra even at room temperature. We demonstrate an enhancement of nonlinear signals by a short pulse excitation, focusing on the optical Kerr effect.

INTRODUCTION

An attractive feature of nanostructures is the great accessibility to single quantum states through their apparent quantization, which enables us to develop unconventional photo functions owing to the flexible controllability of the light–matter interaction [1, 2]. However, the light–matter interaction of a single quantum state is essentially weak because of the localization of their wavefunctions. An effective way for overcoming the small reaction cross-section of a single quantum state is utilizing auxiliary systems such as microcavities or optical antennas made with metallic structures, where the extremely localized photonic modes realize a high probability of excitation of the single quantum states by a few photons [3–5]. The other solution involves the realization of spatially extended quantum states. The large coherent volume due to the collective dipole motions leads to an enhanced oscillator strength [6, 7]. In particular, it has been revealed that one-dimensional confined systems in a nano-to-bulk crossover size regime realize a large light–matter coupling because the wavefunction of confined excitons can match their phase with radiation wave in a medium and their interaction volume becomes extremely large [8–10]. In contrast to the optical responses based on the conventional long-wavelength approximation (LWA) of light, this type of interaction exhibits remarkable optical effects, such as the large radiative shift leading to the interchange of the quantized levels [9] and the ultrafast radiative decay reaching the femtosecond order [10]. Such exciton–radiation coupling beyond LWA strongly modifies the optical spectra relative to those expected only from the bare excitonic systems and interpretation of spectral shape becomes complex. Although a massive number of studies of the excitonic properties in thin film geometry have been performed [11–17], efforts to exploit the potential of the light–matter coupling in a beyond-LWA regime have only just begun, and unresolved physics and potential applications of excitons in promising ma-

terials offer scope for further research.

The nanostructures of ZnO have been attracting the attention of researchers because of their potential applications to innovative optoelectronic devices, such as light-emitting diodes [18, 19], ultraviolet photovoltaics [20], and exciton–polariton lasing [21, 22] utilizing the wide band-gap and large exciton binding energy. Although the formation of a exciton–radiation coupled system is a key to the exploitation of such applications, even the fundamental structures of the coupled modes had been unclear. In recent years, however, we revealed that the radiation-induced coupling between A and B excitons in thin film structures enhances the radiative decay rate of particular exciton–radiation coupled states [23]. This result stimulates us further researches for exploiting coherent nonlinear photo-functions such as ultrafast optical switchings.

In this paper, taking the center-of-mass (c. m.) motions of multicomponent excitons in ZnO, we theoretically show that particular exciton–radiation coupled states exhibit radiative widths over 50 meV and radiative decay times reaching several femto seconds. These values exceed the typical thermal dephasing times at room temperature (10 – 100 fs), and thus, we can expect such modes can effectively survive in the coherent optical signals even at the RT region. Focusing on the optical Kerr response which is a third-order nonlinear optical process, we investigate the pulse width and film thickness dependence of nonlinear signals. The obtained results clearly show that there is an optimal pulse width to enhance the nonlinear intensities for each film thickness.

RADIATIVE DECAY TIME

To reach a full understanding of the optical response of confined excitons, where the interplay between the spatial structures of the radiation field and excitonic waves and their self-consistency should be considered, we first obtain the eigenmodes of an exciton–radiation

coupled system. As a model system, we considered a thin film structure whose thickness direction is along the z -axis. Also, the thickness is assumed to be much thicker than the effective Bohr radius of excitons, and thus, the excitonic relative motions can be treated in the same way as those in bulk system. In this condition, only the c. m. motions of excitons are confined in the sample. According to the standard effective-mass approximation, the eigenenergies of the bare excitons are $E_{\sigma\lambda} = E_{\sigma} + (\hbar^2 k_{\sigma\lambda}^2)/(2M_{\sigma})$, where σ is a band index (thus, σ corresponds to A or B in the case of ZnO), E_{σ} is the energy of transverse excitons in bulk system and M_{σ} is the effective mass of excitons. In order to address the distortion of wavefunctions near the surfaces, we employ the transition layer model [24], and thus, $k_{\sigma\lambda}$ satisfies the following quantized condition: $k_{\sigma\lambda}d - 2 \tan^{-1}(k_{\sigma\lambda}/P_{\sigma}) = \lambda\pi$ ($\lambda = 1, 2, \dots$), where λ is an index of the quantized excitonic state, and P_{σ} is the decay constant of evanescent waves with a value in the order of the inverse of the effective Bohr radius ($P_A = P_B = 1/1.8 \text{ nm}^{-1}$ [25]).

According to the well-known linear response theory [26], the i -th order polarization can be obtained from the perturbation expansion method of the density matrix. Considering a resonant term and multicomponent excitons, the first-order polarization in the site representation $P^{(1)}(z, \omega)$ can be written in nonlocal form as

$$P^{(1)}(z, \omega) = \int dz' \sum_{\sigma\lambda} \frac{|\mu_{\sigma}|^2 g_{\sigma\lambda}(z) g_{\sigma\lambda}^*(z')}{E_{\sigma\lambda} - \hbar\omega - i\Gamma_{\sigma}} E(z', \omega), \quad (1)$$

where Γ_{σ} is a phenomenological damping constant, and $g_{\sigma\lambda}(z)$ is the wavefunction of excitonic c. m. motion. $|\mu_{\sigma}|$ is the transition dipole density for the c. m. confinement regime [27]. Using the retarded Green's function [28], the Maxwell electric field $E(z, \omega)$ in integral form is given as

$$E(z, \omega) = E^{(0)}(z, \omega) + 4\pi q^2 \int dz' G(z, z', \omega) P(z', \omega), \quad (2)$$

where $E^{(0)}(z, \omega)$ is the background electric field. Then we can obtain a closed linear equation system to determine $X_{\sigma\lambda}$ as

$$(E_{\sigma'\lambda'} - \hbar\omega - i\Gamma_{\sigma'}) X_{\sigma'\lambda'} + \sum_{\sigma\lambda} A_{\sigma\sigma'\lambda\lambda'} X_{\sigma\lambda} = F_{\sigma'\lambda'}^{(0)}. \quad (3)$$

In this expression, $F_{\sigma'\lambda'}^{(0)} = \int dz p_{\sigma'\lambda'}^*(z) E^{(0)}(z, \omega)$ indicates an interaction between the exciton and the background electric field, where $p_{\sigma\lambda}(z) = |\mu_{\sigma}| g_{\sigma\lambda}(z)$. $X_{\sigma\lambda} = (E_{\sigma\lambda} - \hbar\omega - i\Gamma_{\sigma})^{-1} \int dz p_{\sigma\lambda}^*(z) E(z, \omega)$ is a solution of eq. (3), which means an amplitude of each

exciton state coupled with radiation, and $A_{\sigma'\sigma\lambda\lambda'}$ describes the radiative correction from the bare exciton state written as

$$A_{\sigma'\sigma\lambda\lambda'}(\omega) = -4\pi q^2 \int \int dz dz' p_{\sigma'\lambda'}^*(z) G(z, z', \omega) p_{\sigma\lambda}(z'), \quad (4)$$

which indicates the radiative coupling between the λ -th σ -band exciton and λ' -th σ' -band exciton via radiation. Describing Eq. (3) in a matrix form as $\mathbf{S}\mathbf{X} = \mathbf{F}^{(0)}$, the eigenmodes of an exciton–radiation coupled system are obtained from $\det|\mathbf{S}| = 0$. The real part $\text{Re}[\hbar\omega_{\xi}]$ gives the eigenenergies including the radiative shift from the bare exciton energies, while the imaginary part $\text{Im}[\hbar\omega_{\xi}]$ gives the radiative widths, where ξ is an index of the quantized exciton–radiation coupled states. Considering the exponential decay of signals, we defined the radiative decay time τ_{ξ} as

$$\tau_{\xi} = \frac{1}{2\text{Im}[\omega_{\xi}]}. \quad (5)$$

In our calculation, we considered the realistic parameters of the A and B excitons in ZnO as shown in Table 1, where m_0 is the static electron mass. By using the two longitudinal exciton energies E_{L1}, E_{L2} and the LT-splitting energies Δ_{LT1} ($= E_{L1} - E_A$), Δ_{LT2} ($= E_{L2} - E_B$), $|\mu_A|$ and $|\mu_B|$ can be written as $|\mu_A|^2 = \epsilon_b \frac{\Delta_{LT1}}{4\pi} \frac{E_{L2} - E_A}{E_B - E_A}$, $|\mu_B|^2 = \epsilon_b \frac{\Delta_{LT2}}{4\pi} \frac{E_B - E_{L1}}{E_B - E_A}$ [23].

TABLE I: Parameters of bulk ZnO [29]

A	B
$M_A = 0.87m_0$	$M_B = 0.87m_0$
$E_A = 3.3758 \text{ eV}$	$E_B = 3.3810 \text{ eV}$
$E_{L1} = 3.3776 \text{ eV}$	$E_{L2} = 3.3912 \text{ eV}$
$\Delta_{LT1} = 1.8 \text{ meV}$	$\Delta_{LT2} = 10.2 \text{ meV}$

OPTICAL KERR RESPONSE

First, we investigate nonlinear optical spectra of A and B excitons in a ZnO thin film, focusing on the optical Kerr response (OKR) which is known as a typical third-order nonlinear optical effect. Figure 1 shows a calculation model of the OKR. The polarization angle of pump light is $\pi/4$ rotated to that of the X-polarized probe light. In the present demonstration, we focus on the dominant contribution, i.e., the effects of the one-exciton resonance while avoiding non-essential issues of two-exciton contributions [23]. It should be noted that the elaborate analysis considering the free two-exciton states through the cancellation effect [30] is necessary for evaluating the absolute values of OKR signals.

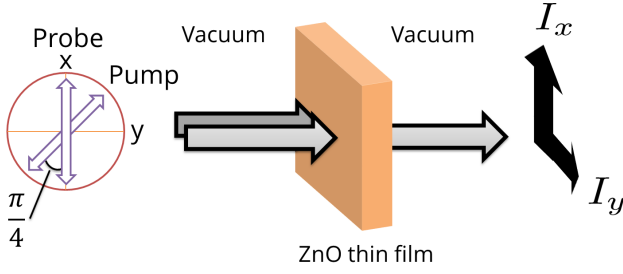


FIG. 1: Calculation model of the optical Kerr response

Considering the first- and third-order polarizations, the total electric field of this configuration can be written as

$$E_{x(y)}(z, \omega) = E_{x(y)}^{(0)}(z, \omega) + \sum_{\sigma} \sum_{\nu} \{X_{\sigma\nu}^{x(y)}(\omega) + U_{\sigma\nu}^{x(y)}(\omega)\} B_{\sigma\nu}(z, \omega), \quad (6)$$

where $E_{x(y)}^{(0)}(z, \omega)$ is the background electric field. Here, we should note that Y-polarized light contains a pure nonlinear component without the background electric field, i. e., $E_y^{(0)}(z, \omega) = 0$. On the other hand, X-polarized light contains both nonlinear and linear components, including background electric field. Also, in this expression, we defined the following values as

$$B_{\sigma\lambda}(z, \omega) = 4\pi q^2 \int dz' G(z, z', \omega) p_{\sigma\lambda}(z'), \quad (7)$$

and

$$U_{\sigma\nu}^{x(y)}(\omega) = \sum_{\lambda} \int \int d\omega_1 d\omega_2 \bar{X}_{\sigma\nu\lambda}(\omega, \omega_1, \omega_2) \times H_{\sigma\nu}^{pump\,x(y)}(\omega_1) H_{\sigma\lambda}^{*pump\,y}((\omega_1 + \omega_2) - \omega) H_{\sigma\lambda}^{probe\,y}(\omega_2). \quad (8)$$

$H_{\sigma\nu}^{pump\,x(y)}(\omega) = \int p_{\sigma\nu}^*(z) \mathcal{E}(z, \omega) dz$ should be determined self-consistently by solving third-order Maxwell's equation. If, however, we assume that an electric field originated from the third-order polarization is much weaker than that originated from the linear polarization, then this value corresponds to the solution of the linear response calculation in a good approximation. $\bar{X}_{\sigma\nu\lambda}(\omega, \omega_1, \omega_2)$ includes energy denominators of triple-resonance to the input frequencies ω_1, ω_2 , and ω written as

$$\bar{X}_{\sigma\nu\lambda}(\omega, \omega_1, \omega_2) = \frac{1}{(\hbar\omega_1 - \hbar\omega - i\gamma_{\sigma})(E_{\sigma\nu} - \hbar\omega - i\Gamma_{\sigma})} \cdot \left\{ \frac{1}{E_{\sigma\lambda} - \hbar\omega_2 - i\Gamma_{\sigma}} + \frac{1}{-E_{\sigma\lambda} + \hbar(\omega_1 + \omega_2 - \omega) - i\Gamma_{\sigma}} \right\} + \frac{1}{(E_{\sigma\nu} - E_{\sigma\lambda} - \hbar\omega + \hbar\omega_2 - i\Gamma_{\sigma})(E_{\sigma\nu} - \hbar\omega - i\Gamma_{\sigma})} \cdot \left\{ \frac{1}{-E_{\sigma\lambda} + \hbar(\omega_1 + \omega_2 - \omega) - i\Gamma_{\sigma}} + \frac{1}{E_{\sigma\nu} - \hbar\omega_1 - i\Gamma_{\sigma}} \right\}, \quad (9)$$

where γ_{σ} is a nonradiative population decay constant.

As an input light, we assume the Gaussian pulses whose integrated intensity of the pump (probe) light is fixed to $3.0 \mu\text{J}/\text{cm}^2$ ($0.3 \text{ nJ}/\text{cm}^2$), and center energies are both 3.378 eV . Here, we considered two kinds of temperature regions, namely, cryogenic temperature (CT) and room temperature (RT), and therefore set corresponding the non-radiative damping parameters as $\Gamma_{\sigma} = \gamma_{\sigma} = 2 \text{ meV}$ and 30 meV .

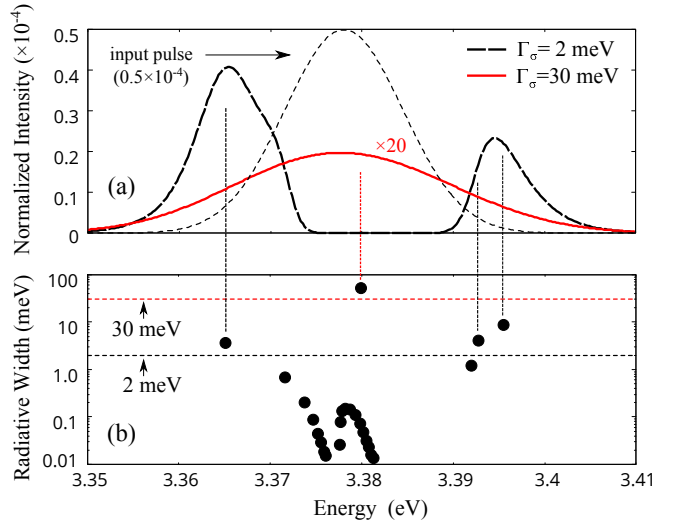


FIG. 2: (a) Γ_{σ} dependence of the optical Kerr spectra $I_y(\omega)$ normalized by a peak intensity of the input probe pulse (the dotted line indicates the spectrum of the input 120-fs probe pulse), and (b) eigenmodes of exciton-radiation coupled system (radiative width vs. eigenenergy) in a film thickness of 291 nm .

Figure 2 shows (a) Γ_{σ} dependence of the optical Kerr spectra $I_y(\omega)$ of a ZnO thin film normalized by a peak intensity of the input probe pulse $I_y(\omega)$, and (b) eigenmodes of exciton-radiation coupled system (radiative width vs. eigenenergy) in a film thickness of 291 nm . The input 120-fs pulses can cover a certain range of spectral width and excite the lower, middle, and upper branches of exciton-radiation coupled modes at once. We find that the energy and spectral width of the signals obviously reflect the eigenenergies and radiative widths of eigenmodes. In the case $\Gamma_{\sigma} = 2 \text{ meV}$ (CT

region), the eigenmodes with radiative widths greater than 2 meV dominantly appear, and thus, large splitting between the lower and upper signals is clear in the spectrum. On the other hand, the eigenmodes with radiative widths narrower than 2 meV are less reflected in the spectrum because of the damping effect. Here, each of two peaks at CT should not be attributed solely to the A or B exciton from their energy position. It should be noted that these two peaks should be assigned to respective mixed modes containing both A and B excitons due to the radiative coupling [23].

With an increase in thermal damping Γ_σ , these two peaks disappear, and only one mode with a very broad spectral width appears (red line). The radiative width of this mode is in excess of 50 meV, and thus, a large nonlinear signal can survive even at $\Gamma_\sigma = 30$ meV (RT region) because the coherent response is faster than the dephasing under this condition.

In above discussions, however, the 120-fs input pulse may not be so effective to maximize the nonlinear intensity because it cannot cover the broad radiative width of the fastest mode. Also, we can expect there must be dependences of the input pulse width and the film thickness on the output nonlinear intensities. In the next section, we investigate how to maximize the nonlinear intensities by changing these parameters.

NONLINEAR EFFICIENCY

In order to evaluate the intensity of OKR signals, we defined the nonlinear efficiency η as a ratio of the integrated intensity of the input probe light and output Y-polarized one as

$$\eta = \frac{\int I_y(\omega)d\omega}{\int I_{probe}(\omega)d\omega}. \quad (10)$$

Figure 3 shows the pulse width dependence of the nonlinear efficiency η in a film thickness 291 nm. The

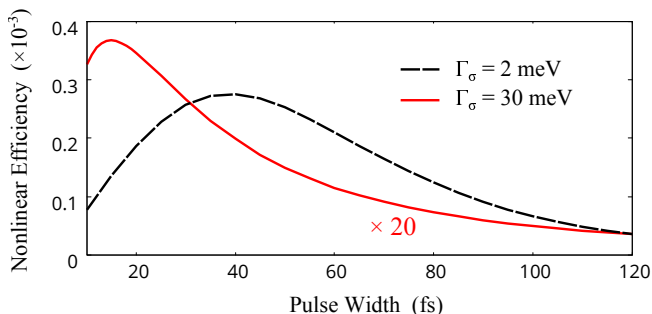


FIG. 3: Pulse width dependence of the nonlinear efficiency η in a film thickness of 291 nm.

value of η becomes maximum when the input pulse effectively cover the peak structures shown in Fig. 2 (a). In the case $\Gamma_\sigma = 2$ meV (CT region), the upper and lower modes are relatively dominant compared with the fastest decay mode. Therefore nearly 40 fs pulses become optimal, although too short pulses are not effective because of the loss of energy.

On the other hand, in the case $\Gamma_\sigma = 30$ meV (RT region), the fastest decay mode with the radiative width over 50 meV (the radiative decay time reaching several femto seconds) dominantly survives in the optical responses. In this situation, shorter inputs with nearly 15 fs pulse width are effective to cover the very broad radiative width of this mode. The nonlinear efficiency is about 10 times enhanced compared with that of the 120 fs pulse excitation. An significant point is that the high damping does not much reduce the nonlinear efficiency although the damping is fifteen times greater than that at CT, especially in the case of nearly 15 fs pulses. This is because the radiative width is much broader than Γ_σ and less affected by the thermal damping effects.

From these results, we can expect a compatibility between fast and strong nonlinear responses by short pulse excitation at the RT region. Then, we demonstrate it by comparing the radiative decay time τ_ξ and the nonlinear efficiency η . Figure 4 shows the film thickness dependences of (a) τ_ξ and (b) η with some pulse widths in $\Gamma_\sigma = 30$ meV. We found two particularly noteworthy points in these figures. (1) An optimal pulse width depends on the film thickness. This is because the radiative width of the coupled mode is determined from the interaction volume (film thickness) between excitons and radiation field. Therefore, when the radiative decay times become much shorter than the input pulse width with a increase of the film thickness, the nonlinear efficiency decreases conversely. (2) In the case of the 10 fs pulse, similarly to the tendency with radiative decay times, the nonlinear efficiency increases with the film thickness. In particular, the local minimal values of the radiative widths and maximal values of the nonlinear intensity occur at around the same thickness, which indicates the fast radiative decay of excitons becomes compatible with sufficient nonlinear responses if we choose an appropriate film thickness and input pulse width.

It should be noted that, for a thickness region of less than 80 nm, the nonlinear efficiency is quite weak. However, around this thickness where the radiative decay speed exceeds that of dephasing, the growth of the nonlinear efficiency becomes rapid even in the case of $\Gamma_\sigma = 30$ meV. For ZnO, this occurs in relatively thin regions because of the formation of wider radiative widths owing to the radiative coupling of the A and B excitons.

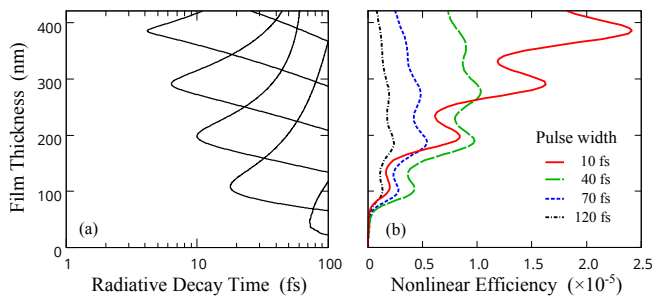


FIG. 4: Film thickness dependence of (a) the radiative decay time τ_ξ , and (b) the nonlinear efficiency η with some pulse widths in $\Gamma_\sigma = 30$ meV.

CONCLUSION

In this paper, taking the A and B excitons in ZnO, we have theoretically investigated the exciton–radiation coupled modes and their nonlinear optical responses focusing on the optical Kerr effect. Because of the large radiative coupling of excitons, particular modes exhibit huge radiative widths over 50 meV (short radiative decay times reaching several femto seconds) which can exceed the thermal damping at room temperature. That is why such modes survive in the optical Kerr signals even assuming damping parameters at RT region. Then, we demonstrated the input pulse width dependence of nonlinear efficiencies which is considered to increase when the input pulses effectively cover the broad radiative widths. As a result, we have found that the optimal short pulses enhance the nonlinear efficiency with sufficient values even at RT, compared with those at CT. Furthermore, the film thickness dependence of the radiative decay times and nonlinear efficiencies clearly shows the possibility of compatibility between the fast and strong nonlinear responses by choosing an appropriate film thickness and input pulse width. This is in contrast to the conventional observation of the optical responses of excitons where a coherent nonlinear response is never prominent at RT because the thermal dephasing is much faster than the typical population decay of excitons.

The authors thank Professor M. Nakayama, Professor M. Ashida, Professor M. Ichimiya, and Professor N. Yokoshi for their fruitful discussions. This work was partially supported by a Grant-in-Aid for Scientific Research (A) No. 24244048 from Japan and by the Japan Society for Promotion of Science (JSPS).

[1] T. Meier, P. Thomas, and S. W. Koch, *Coherent Semiconductor Optics: From Basic Concepts to Nanostructure Applications* (Springer, 2007).

[2] V. I. Gavrilenko, *Optics of Nanomaterials* (Pan Stanford Publishing Pte. Ltd., 2011).

[3] J. Kasprzak, M. Richard, S. Kundermann, A. Baas, P. Jeambrun, J. M. J. Keeling, F. M. Marchetti, M. H. Szymańska, R. André, J. L. Staehli, V. Savona, P. B. Littlewood, B. Deveaud, and L. S. Dang, *Nature* **443**, 409 (2006).

[4] Y. F. Xiao, Y. C. Liu, B. B. Li, Y. L. Chen, Y. Li, and Q. Gong, *Phys. Rev. A* **85**, 031805 (R) (2012).

[5] Y. Osaka, N. Yokoshi, M. Nakatani, and H. Ishihara, *Phys. Rev. Lett.* **112**, 133601 (2014).

[6] E. Hanamura, *Phys. Rev. B* **38**, 1228 (1988).

[7] T. Takagahara, *Phys. Rev. B* **47**, 16639 (1993).

[8] H. Ishihara, K. Cho, K. Akiyama, N. Tomita, Y. Nomura, and T. Isu, *Phys. Rev. Lett.* **89**, 017402 (2002).

[9] A. Syouji, A. P. Zhang, Y. Segawa, J. Kishimoto, H. Ishihara, and K. Cho, *Phys. Rev. Lett.* **92** 257401 (2004).

[10] M. Ichimiya, M. Ashida, H. Yasuda, H. Ishihara, and T. Itoh, *Phys. Rev. Lett.* **103**, 257401 (2009).

[11] R. Del Sole, and A. D’Andrea, *Excitons in Thin Films, H. Haug, and L. Bányai, Optical Switching in Low-Dimensional Systems, 194, 289-300 (NATO ASI Series 1989).*

[12] G. S. Agarwal, D. N. Pattanayak, and E. Wolf, *Phys. Rev. Lett.* **27**, 1022 (1971).

[13] K. Cho, and M. Kawata, *J. Phys. Soc. Jpn.* **54**, 4431 (1985).

[14] K. Cho, and H. Ishihara, *J. Phys. Soc. Jpn.* **59**, 754 (1990).

[15] A. Tredicucci, Y. Chen, F. Bassani, J. Massies, C. De-paris, and G. Neu, *Phys. Rev. B* **47**, 10348 (1993).

[16] I. V. Belousov, J. B. Ketterson, and Y. Sun, *Phys. Rev. B* **81**, 205208 (2010).

[17] B. Foy, E. McGlynn, A. Cowley, P. J. McNally, and M. O. Henry, *J. Appl. Phys.* **112**, 033505 (2012).

[18] M. Chen, M. P. Lu, Y. Wu, J. Song, C. Lee, M. Y. Lu, Y. Chang, L. Chou, Z. Wang, and L. Chen, *Nano. Lett.* **10** 4387 (2010).

[19] X. Li, J. Qi, Q. Zhang, Q. Wang, F. Yi, Z. Wang, and Y. Zhang, *Appl. Phys. Lett.* **102**, 221103 (2013).

[20] J. J. Cole, X. Wang, R. J. Knuesel, and H. O. Jacobs, *Nano. Lett.* **8**, No. 5 1477 (2008).

[21] L. Orosz, F. Réveret, F. Médard, P. Disseix, J. Leymarie, M. Mihailovic, D. Solnyshkov, G. Malpuech, J. Zuniga-Pérez, F. Semon, M. Leoux, S. Bouchoule, X. Lafosse, M. Mexis, C. Brimont, and T. Guillet, *Phys. Rev. B* **85** 121201 (2012).

[22] F. Li, L. Orosz, O. Kamoun, S. Bouchoule, C. Brimont, P. Disseix, T. Guillet, X. Lafosse, M. Leroux, J. Leymarie, G. Malpuech, M. Mexis, M. Mihailovic, G. Patriarce, F. Réveret, D. Solnyshkov, and J. Zuniga-Perez, *Appl. Phys. Lett.* **102**, 191118 (2013).

[23] T. Kinoshita and H. Ishihara, to be accepted.

[24] A. D’Andrea, and R. Del Sole, *Phys. Rev. B* **25**, 3714 (1982).

[25] C. Klingshirn, *Phys. Stat. Sol. (b)* **244**, 3027 (2007).

[26] R. Kubo, and K. Tomita, *J. Phys. Soc. Jpn.* **9**, 888 (1954).

[27] Y. Ohfuti and K. Cho, *Phys. Rev. B*, **51**, 14379 (1995).

[28] W. C. Chew: *Waves and Fields in Inhomogeneous Media* (Wiley-IEEE PRESS, 1995).

[29] J. Lagois, *Phys. Rev. B* **23**, 5511 (1981).

[30] H. Ishihara, and K. Cho, *Phys. Rev. B* **42**, 1724 (1990).